The skeletal isomerization of 1-butene over Zn-silicoaluminophosphate molecular sieves

D. Escalante, B. Méndez, G. Hernández, C.M. López, F. J. Machado, J. Goldwasser * and M.M. Ramírez de Agudelo [a]

Centro de Catálisis, Petróleo y Petroquímica, Escuela de Química, Facultad de Ciencias, Universidad Central de Venezuela, Apartado Postal 47102, Los Chaguaramos, Caracas 1020-A, Venezuela
E-mail: jgoldwas@strix.ciens.ucv.ve
[a] *INTEVEP, SA, Apartado 76343, Caracas 1070-A, Venezuela*

Received 2 April 1997; accepted 16 July 1997

The catalytic transformations of 1-butene were performed over a zinc-substituted silicoaluminophosphate molecular sieve (ZnAPSO-11), over a Zn-supported SAPO-11 molecular sieve (Zn/SAPO-11) and over the unpromoted SAPO-11 solid. The ZnAPSO-11 catalyst showed the highest selectivity towards skeletal isomerization as well as the highest skeletal isomerization efficiency (SIE). In addition, the largest number of acid sites, particularly strong acid sites, were observed with temperature-programmed desorption of ammonia (NH_3-TPD) over the ZnAPSO-11 catalyst. The acid strength over the latter was also the highest. The agreement between the catalytic and the acidity results obtained in the present work can be explained in terms of the model of Gielgens et al. In this model, the substitution of Al(III) ions by Zn(II) ions leads to partially unsaturated Zn(II) ions in the vicinity of structural P–OH groups. The Brønsted acidity of the latter may be enhanced by Brønsted–Lewis interaction, thus rendering catalysts with stronger acidity necessary for the skeletal isomerization. The lower molar fraction of Al(III) cations found in the ZnAPSO-11 solid, compared to the SAPO-11 sample, strongly supports the above. The results for the Zn-supported system were extremely different. Significant decreases in the strong acidity as well as in the skeletal isomerization selectivity, compared to the ZnAPSO-11 catalyst, were observed. These differences reinforce the idea of incorporation of Zn(II) into the silicoaluminate framework for the ZnAPSO-11 solid.

Keywords: 1-butene, skeletal isomerization, Zn-silicoaluminophosphates

1. Introduction

The skeletal isomerization of *n*-butenes has been the subject of detailed studies over a variety of catalytic systems for over 30 years [1–7]. Different reaction mechanisms have been proposed [1,2,4–7] in the literature. Besides the significant academic implications involved in this reaction, its industrial importance is well established due to the new requirements for reformulated gasolines. The latter includes the reduction of volatile compounds (particularly, C_4 and C_5), the decrease in the amount of olefins present in gasoline and the addition of oxygenated compounds, which can act as octane enhancers. Among different oxygenated products, methyl tert-butyl ether (MTBE), has been proven [7,8] as a valuable octane booster oxygenated fuel additive. Since MTBE is industrially obtained from the reaction of methanol with isobutene, the relevance of highly selective catalysts for the skeletal isomerization of *n*-butenes is evident.

Metal-substituted aluminophosphates (MeAPO's) [3,9,10], silicoaluminophosphates (SAPO's) and metal-substituted silicoaluminophosphates (MeAPSO's) [11–13] are among the catalytic systems reported active for the skeletal isomerization of 1-butene. The high selectivity shown for the formation of isobutene over these solids has been associated with a characteristic acid site distribution and a particular crystal topology which minimize cracking and oligomerization side reactions.

Yang et al. [3] studied a series of MeAPO's for the skeletal isomerization of 1-butene. High selectivities for the latter were observed over Co-, Zn- and Mn-substituted aluminophosphates. Recently, we reported [10] an increase in the acidity of a series of substituted MeAPO's (Me = Mn, Cr, Fe), which caused an increase in the selectivity towards isobutene, compared to the unsubstituted $AlPO_4$-11 matrix. Different substitution models, depending on the metal oxidation state and stability of the metal species in the framework, were proposed to account for the results. In particular, for a divalent cation (Mn(II)), the model advanced by Gielgens et al. [9] was used to explain the increase in acidity observed when the metal was incorporated into the aluminophosphate structure. In a recent study, Elangovan et al. [14] reported the incorporation of zinc into the structures of an $AlPO_4$-5 and $AlPO_4$-11 molecular sieves. These authors observed an increase in acidity as well as an increase in the unit cell volume for the substituted $ZnAPO_4$'s in comparison with the unsubstituted materials.

* To whom correspondence should be addressed.

Since the preferred oxidation state of the zinc cation is 2+, we decided, in terms of our early data [10] and other results [3,9,14], to study the skeletal isomerization of 1-butene over a substituted (ZnAPSO-11) and supported (Zn/SAPO-11) zinc-silicoaluminophosphate molecular sieves. Temperature-programmed desorption of ammonia (NH_3-TPD) was carried out in order to establish a possible link with the skeletal isomerization selectivities. The results will be discussed in terms of the possible mechanism of incorporation of zinc into the molecular sieve structure.

2. Experimental

2.1. Catalysts

The synthesis procedure for the SAPO-11 has been reported elsewhere [15]. The SAPO-11 catalyst used in the present work was prepared similarly to sample S-2 (table 1) of ref. [15]. The molar composition formula TO_2 of the calcined solid was $(Al_{0.48}P_{0.47}Si_{0.05})O_2$. The specific surface area (SSA) and the micropore volume were 126 m^2/g and 0.038 cm^3/g, respectively.

The synthesis of the ZnAPSO-11 was performed according to the following scheme: The alumina source (pseudoboehmite, Catapal B from Vista Chemical Co.) was added to a diluted solution of phosphoric acid (Aldrich), and the mixture was stirred for 2 h. Thereafter, the source of silicon (40% SiO_2 colloidal silica, Ludox AS40 from Dupont) was added, and the mixture stirred again for 2 h. The zinc promoter (Zn(II) nitrate hexahydrate (Aldrich)) was then incorporated, followed by a stirring period of 2 h. The final step was the addition of the organic template (di-*n*-propylamine (DPA) (Aldrich)), which was followed by a stirring period of 2 h. The gel molar composition was: $0.9Al_2O_3{:}P_2O_5{:}0.2ZnO{:}DPA{:}40H_2O{:}0.3SiO_2$. A final crystallization temperature of 473 K and a crystallization time of 24 h were employed. The solid was first washed with distilled water and dried at 383 K for 16 h. The catalyst was then calcined under dry air at 813 K for 15 h in order to remove organic residues. The molar composition formula for the calcined solid was $(Al_{0.44}P_{0.46}Zn_{0.052}Si_{0.051})O_2$. The SSA and microporous volume for the ZnAPSO-11 sample were 129 m^2/g and 0.039 cm^3/g, respectively. A supported Zn/SAPO-11 catalyst was prepared by impregnating a sample of SAPO-11 with the same zinc promoter using the incipient wetness technique. The Zn wt% was 1.9. The SSA for this sample was 72 m^2/g while the microporous volume was 0.023 cm^3/g.

2.2. Procedures

X-ray diffractograms were recorded with a Philips diffractometer PW 1730 using Co Kα radiation ($\lambda = 1.790255$ Å) operated at 30 kV, 20 mA and scanning speed of 2° (2θ/min). For more details see ref. [15].

Specific surface areas and micropore volumes were determined on a commercial Micromeritics ASAP 2400 surface area analyzer at liquid-nitrogen temperature.

NH_3-TPD was carried out with the aid of a Micromeritics 2900 TPD/TPR apparatus. Samples were pretreated under dry nitrogen flow by increasing the temperature from ambient to 513 K, at a heating rate of 2 K/min. After 30 min at 513 K, the temperature was increased up to 813 K, at a rate of 5 K/min. The catalyst was left for 1 h at 813 K. The sample was then cooled down to 403 K and pulses of dry NH_3 were passed over the catalyst, using He as the carrier gas. After saturation, the chemisorbed ammonia was desorbed in the following way: Firstly, by heating the sample from 403 to 493 K at a heating rate of 10 K/min. Then, the sample was kept isothermally at 493 K for 15 min. Finally, the temperature was raised at the same heating rate to 813 K until the desorption was completed.

Catalytic experiments were performed in a conventional continuous flow system [10,12,16] operated at atmospheric pressure. The methodology used is identical to that described in ref. [16], but will be repeated here for the sake of completion. Preliminary experiments were carried out to determine the reaction conditions for maximum steady-state formation of isobutene. The reaction parameters used were: reaction temperature = 743 K, N_2 flow = 60 cm^3/min, 1-butene flow = 15 cm^3/min, weight of catalyst = 1 g. The reaction products were analyzed by on-line gas chromatography, using a Hewlett-Packard 5890 chromatograph with a flame ionization detector. A fused silica KCl/Al_2O_3 column was used for separation purposes. The catalytic tests were performed, for the calcined catalysts, after the solids were pretreated in situ (N_2, 60 cm^3(STP)/min) overnight.

2.3. Data treatment

For a reaction product (or set of products), the selectivity is defined by

$$S_i = \left\{ A_i / \left(\sum A_i \right) - A_{1\text{-butene}} \right\} \times 100 , \qquad (1)$$

where A_i is the corrected chromatographic area for a particular compound. The following selectivities were determined: S_{iso} (skeletal isomerization), $S_{2\text{-b}}$ (double-bond isomerization), S_{diene} (formation of butadiene), S_{crack} (formation of C_1–C_3 products), $S_{C_{5+}}$ (formation of hydrocarbons with 5 or more carbon atoms). S_{crack} and $S_{C_{5+}}$ were calculated by including the sum of the corresponding hydrocarbon areas in the numerator of eq. (1).

The total conversion (X) was calculated according to

$$X = \left\{ \left(\sum A_i \right) - A_{1\text{-butene}} / \sum A_i \right\} \times 100 . \qquad (2)$$

The skeletal isomerization efficiency (SIE) is defined by

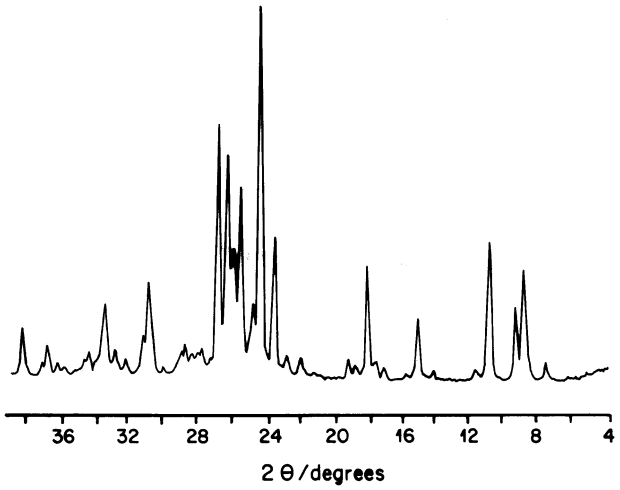

Figure 1. X-ray diffractogram of the as-synthesized ZnAPSO-11 catalyst.

$$\mathrm{SIE} = \{A_{\mathrm{isobutene}}/(A_{\mathrm{isobut}} + A_{\mathrm{cis\text{-}2\text{-}but}} + A_{\mathrm{trans\text{-}2\text{-}but}}) \times 0.467\} \times 100\,, \quad (3)$$

the 0.467 term corresponds to the isobutene equilibrium fraction at 743 K.

2.4. Reagents

1-butene was Matheson C.P. grade. Ammonia (Matheson) was dried by passing it over activated molecular sieve traps to remove traces of water. For further experimental details, see ref. [15].

3. Results and discussion

Figure 1 shows the XRD diffractogram for the as-synthesized ZnAPSO-11 sample. The solid is pure and highly crystalline with $AlPO_4$-11 (AEL) structure, in agreement with the literature [15–17]. The XRD results for the Zn/SAPO-11 system were similar to those reported for the SAPO-11 support [15].

Ammonia TPD profiles for SAPO-11, ZnAPSO-11 and for Zn/SAPO-11 are presented in figure 2. The amount of desorbed ammonia as a function of the temperature is shown in table 1. It can be readily observed that the total acidity, measured as the total amount (mmol/g_{cat}) of ammonia desorbed, is larger for the ZnAPSO-11 sample than for the other two catalysts. The amount of ammonia desorbed during the high-temperature ramp is also considerably higher. Furthermore, the high-temperature peak showed a maximum at around 703 K for the ZnAPSO-11 sample, compared to 624 K for the Zn/SAPO-11 solid and 621 K for the SAPO-11 sample. These results indicate a larger number of acid sites as well as an increase in the acid strength for the ZnAPSO-11 solid.

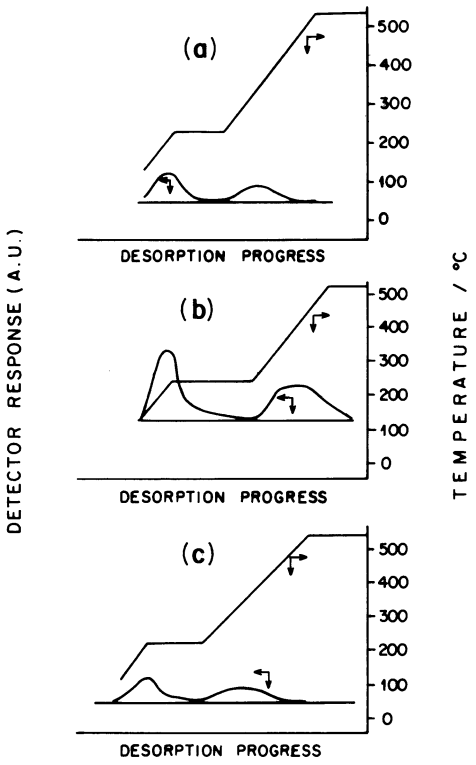

Figure 2. Ammonia-TPD profiles for : (a) SAPO-11, (b) ZnAPSO-11, and (c) Zn/SAPO-11.

The differences in acidity shown can be accounted for in terms of the incorporation of Zn(II) into the silicoaluminophosphate structure (ZnAPSO-11) by repla-

Table 1
Ammonia-TPD data

Catalyst	Total acidity [a] (mmol of NH_3/g_{cat})	T_1 [b] (K)	T_2 [c] (K)	mmoles NH_3/g_{cat} [d]	
				(403–493 K)	(493–813 K)
SAPO-11	0.64	495	621	0.40	0.24
ZnAPSO-11	1.3	508	703	0.40	0.90
Zn/SAPO-11	0.40	499	624	0.23	0.17

[a] Total acidity, expressed as mmol of ammonia per gram of catalyst desorbed within the 403–813 K temperature range.
[b] Temperature at peak maximum (low-temperature peak).
[c] Temperature at peak maximum (high-temperature peak).
[d] mmol of ammonia per gram of catalyst desorbed in each temperature range.

cement of an Al(III) cation, according to the model of Gielgens et al. [9]. According to the latter, Zn(II) would be incorporated into the molecular sieve framework generating one P–OH group per each metal ion, thus increasing the number of acid sites. The interaction of the metal ions (Lewis centers) with the P–OH groups (Brønsted sites) may increase the strength of the latter, as shown for related systems [16,18–20]. The replacement of Al(III) by Zn(II) cations is strongly supported by the TO_2 formulas for SAPO-11 and ZnAPSO-11 solids. As observed (see experimental section), the Al(III) molar fraction is lower in the latter (0.44) than in the former (0.48), by an amount very close to the molar fraction of incorporated zinc.

The catalytic results reported in tables 2–4 are consistent with the acidity measurements. The three solids showed similar total conversions throughout the catalytic runs. The ZnAPSO-11 catalyst, however, was the most selective catalyst towards the formation of isobutene. The skeletal isomerization efficiency (SIE) reached 100% for the ZnAPSO-11 after 0.5 h, viz., the production of isobutene is thermodynamically controlled over this catalytic system. As observed (tables 2 and 3), the double-bond isomerization is favored over the SAPO-11 solid compared to the ZnAPSO-11 catalyst. It has been reported [21,22] that double-bond shift is a facile reaction which requires weak acid sites while the skeletal isomerization is much more demanding, requiring stronger acid sites. Thus, the increase in the number of strong acid sites, as well as the increase in the strength of the latter, may account for the higher selectivity for the skeletal isomerization reaction, at the expense of the 2-butenes, observed for the ZnAPSO-11 compared to the SAPO-11 sample. At higher TOS, the S_{iso} for the ZnAPSO-11, as well as the S_{crack} and $S_{C_{5+}}$, decrease while the selectivity towards double-bond isomerization increases. This can be understood in terms of progressive poisoning of a fraction of the strong acid sites (created by the incorporation of Zn(II) into the molecular sieve framework) by carbonaceous residues, since cracking and oligomerization reactions also need strong acid sites to take place.

The results for the Zn/SAPO-11 catalyst are extremely different (table 4). The selectivity towards skeletal isomerization is much lower (at best 10.7%), while the double-bond isomerization is favored compared to the ZnAPSO-11 and SAPO-11 materials. These results agree, in terms of the above discussion, with the lower number of strong acid sites and the decrease in the acid strength (table 1) observed for this solid, compared to the ZnAPSO-11 catalyst. The Zn-supported system also showed a lower number of total acid sites compared to the SAPO-11 sample. The acid strength (similar desorption temperatures) as well as the acid distribution were, however, similar for these two systems. Seemingly, the impregnation of Zn(II) ions reduces the number of total acid sites, probably by pore plugging caused by non-framework species, in agreement with other results [10,16]. The latter is supported by the decrease observed in the micropore volume ($\sim 40\%$) of this solid compared to that of SAPO-11. The low number of strong acid sites on the supported catalyst is probably responsible for the low values of S_{iso}, $S_{C_{5+}}$ and S_{crack} observed for this system.

Finally, previous experiments [13], carried out under the same experimental conditions as used in the present work, have shown that an $AlPO_4$-11 (sample A-0, ref. [15]) catalyst was about five times less selective towards skeletal isomerization than the corresponding ZnAPO-11 solid. Other data [3] have indicated that at 673 K for a ZnAPO-11 catalyst, the skeletal isomerization selectivity was about three times higher than that found over the $AlPO_4$-11 counterpart. These results support the above discussion in terms of incorporation of Zn(II) into the molecular sieve framework. It should be noted, however, that our data shows ([13] and table 3), that the skeletal isomerization selectivity for the

Table 3
Product distribution for the transformation of 1-butene over ZnAPSO-11

Time on stream (h)	X	S_{iso}	$S_{2\text{-b}}$	S_{diene}	$S_{C_{5+}}$	S_{crack}	SIE
0.50	78.0	43.0	49.0	0.0	4.0	4.0	100.0
1.50	81.0	37.3	57.9	0.0	2.6	2.2	84.0
2.50	80.3	35.5	60.5	0.0	2.1	1.9	79.4
3.50	80.4	35.0	61.4	0.0	1.8	1.7	77.9
4.50	79.6	34.2	62.1	0.0	1.9	1.8	76.2
5.50	79.6	33.2	63.5	0.0	1.8	1.5	73.7
6.50	79.1	32.4	64.4	0.0	1.6	1.6	71.8

Table 2
Product distribution for the transformation of 1-butene over SAPO-11

Time on stream (h)	X	S_{iso}	$S_{2\text{-b}}$	S_{diene}	$S_{C_{5+}}$	S_{crack}	SIE
0.50	77.6	24.0	70.6	0.0	2.3	3.1	54.5
1.50	77.4	24.0	71.4	0.0	1.7	2.9	54.0
2.50	77.1	23.7	71.9	0.0	1.8	2.7	53.2
3.50	76.7	23.6	72.2	0.0	1.8	2.3	52.8
4.50	76.7	23.2	72.9	0.0	1.6	2.3	51.8
5.50	76.5	23.0	73.5	0.0	1.4	2.2	51.1
6.50	76.4	22.8	73.8	0.0	1.3	2.1	50.6

Table 4
Product distribution for the transformation of 1-butene over Zn/SAPO-11

Time on stream (h)	X	S_{iso}	$S_{2\text{-b}}$	S_{diene}	$S_{C_{5+}}$	S_{crack}	SIE
0.50	79.4	10.7	87.4	0.2	0.7	0.9	23.5
1.50	77.9	8.5	89.8	0.3	0.8	0.6	18.7
2.50	70.7	10.2	88.0	0.4	0.7	0.8	22.2
3.50	77.1	5.9	92.8	0.3	0.4	0.5	12.9
4.50	76.8	5.3	93.5	0.3	0.4	0.5	11.5
5.50	65.9	8.0	90.2	0.5	0.5	0.7	17.4
6.50	76.6	4.1	95.0	0.3	0.2	0.4	8.8

ZnAPO-11 sample is much lower than that for the ZnAPSO-11 solid. This can be understood in terms of the incorporation of Si into the molecular sieve framework, as suggested previously [10,13,15]. The strong acid sites brought about by the incorporation of Si add up to the Zn-generated acid sites discussed earlier, rendering catalysts more selective towards the skeletal isomerization of 1-butene.

4. Conclusions

The catalytic transformations of 1-butene were performed over a zinc-substituted silicoaluminophosphate molecular sieve (ZnAPSO-11), over a Zn-supported SAPO-11 molecular sieve (Zn/SAPO-11) and over the unpromoted SAPO-11 sample. The data indicate a higher skeletal isomerization selectivity for the ZnAPSO-11 solid. This result agrees with the stronger acidity observed for this catalyst. The results obtained in the present work can be explained in terms of the model of Gielgens et al. [9], where the substitution of Al(III) ions by Zn(II) ions leads to partially unsaturated Zn(II) ions in the vicinity of structural P–OH groups. The Brønsted acidity of the latter may be enhanced by Brønsted–Lewis interaction, as observed for related systems. The lower molar fraction of Al(III) cations found in the ZnAPSO-11 solid, compared to the SAPO-11 sample, strongly supports the above.

The results for the Zn-supported system were extremely different. Significant decreases in the strong acidity as well as in the skeletal isomerization selectivity, compared to the ZnAPSO-11 catalyst, were observed. These differences reinforce the idea of incorporation of Zn(II) into the silicoaluminate framework for the ZnAPSO-11 solid.

Acknowledgement

The authors would like to express their gratitude to Consejo Nacional de Investigaciones Científicas y Tecnológicas (CONICIT) for financial support, through grant RPI-10001.

References

[1] D.M. Brouwer and J.M. Oelderik, Rec. Trav. Chim. Pays Bas 87 (1968) 721.
[2] V.R. Choudhary, Chem. Ind. Dev. 8(7) (1974) 32.
[3] S.M. Yang, D.H. Guo, J.S. Lin and G.T. Wang, in: *Zeolites and Related Microporous Materials: State of the Art 1994*, Studies in Surface Science and Catalysis, Vol. 84, eds. J. Weitkamp, H.G. Karge, H. Pfeifer and W. Hölderich (Elsevier, Amsterdam, 1994) p. 1677.
[4] M. Asensi, A. Corma and A. Martínez, J. Catal. 158 (1996) 561.
[5] Z.X. Cheng and V. Ponec, J. Catal. 148 (1995) 607;
M. Guisnet, P. Andy, G. Gnep, E. Benazzi and C. Travers, J. Catal. 158 (1996) 551.
[6] H.H. Mooiweer, K.P. de Jong, B. Kraushaar-Czarnetzki, W.H.J. Stork and B.C.H. Krutzen, in: *Zeolites and Related Microporous Materials: State of the Art 1994*, Studies in Surface Science and Catalysis, Vol. 84, eds. J. Weitkamp, H.G. Karge, H. Pfeifer and W. Hölderich (Elsevier, Amsterdam, 1994) p. 2327.
[7] M.W. Simon, S.L. Suib and C.-L. O'Young, J. Catal. 147 (1994) 484.
[8] I.E. Maxwell and J.E. Naber, Catal. Lett. 12 (1992) 105.
[9] L.H. Gielgens, I.H.E. Veenstra, V. Ponec, M.J. Haanepen and J.H.C. van Hooff, Catal. Lett. 32 (1995) 195.
[10] D. Arias, I. Campos, D. Escalante, J. Goldwasser, C.M. López, F.J. Machado, B. Méndez, D. Moronta, M. Pinto, V. Sazo and M.M. Ramírez de Agudelo, J. Mol. Catal., in press.
[11] H.-L. Zubowa, M. Richter, U. Roost, B. Parlitz and R. Fricke, Catal. Lett. 19 (1993) 67;
G.J. Gajda, US Patent 5132484 (1991).
[12] D. Escalante, C.M. López, F.J. Machado, M. Matjushing, B. Méndez, M. Pinto and M.M. Ramírez-Agudelo, in: *Environmental Catalysis*, eds. G. Centi, C. Cristiani, P. Forzatti and S. Perathoner (SCI, Rome, 1995) p. 415.
[13] D. Escalante, J. Goldwasser, C.M. López, F.J. Machado, M. Pinto and M.M. Ramírez-Agudelo, in: *Proc. XV Iberoamerican Symp. on Catalysis*, Vol. 1, Córdoba 1996, eds. E. Herrero, O. Anunziata and C. Pérez, p. 103.
[14] S.P. Elangovan, V. Krishnasamy and V. Murugesan, Catal. Lett. 36 (1996) 271.
[15] M. Alfonzo, J. Goldwasser, C.M. López, F.J. Machado, M. Matjushin, B. Méndez and M.M. Ramírez de Agudelo, J. Mol. Catal. 98 (1995) 35.
[16] D. Escalante, L. Giraldo, M. Pinto, C. Pfaff, V. Sazo, M. Matjushin, B. Méndez, C.M. López, F.J. Machado, J. Goldwasser and M.M. Ramírez de Agudelo, J. Catal., in press.
[17] E.M. Flanigen, B.M.T. Lok, R.L. Patton and S.T. Wilson, US Patent 4738837 (1988).
[18] U. Cornaro, P. Jiru, Z. Tvaruzkova and K. Habersberger, in: *Zeolite Chemistry and Catalysis*, eds. P.A. Jacobs, N.I. Jaeger and L. Kubelkova (Elsevier, Amsterdam, 1991) p. 165.
[19] J. Jänchen, M.P.J. Peeters, J.H.M.C. van Wolput, J.P. Wolthuizen, J.H.C. van Hooff and U. Lohse, J. Chem. Soc. Faraday Trans. 90 (1994) 1033.
[20] J.D. Chen and R.A. Sheldon, J. Catal. 153 (1995) 1.
[21] A. Corma and B. Wojciechowski, Catal. Rev. Sci. Eng. 24 (1982) 1.
[22] C.-L. O'Young, W.-Q. Xu, M. Simon and S.L. Suib, in: *Zeolites and Related Microporous Materials: State of the Art 1994*, Studies in Surface Science and Catalysis, Vol. 84, eds. J. Weitkamp, H.G. Karge, H. Pfeifer and W. Hölderich (Elsevier, Amsterdam, 1994) p. 1671.